Published in final edited form as:
Pigment Cell Melanoma Res. 2009 October ; 22(5): 611–622. doi:10.1111/j.1755-148X.2009.00584.x.

Comparison of melanoblast expression patterns identifies distinct classes of genes

Stacie K. Loftus[*], **Laura L. Baxter**, **Kristina Buac**, **Dawn E. Watkins-Chow**, **Denise M. Larson**, and **William J. Pavan**
National Institutes of Health, National Human Genome Research Institute, Genetic Disease Research Branch, Bethesda MD, 20892, USA

Summary

A full understanding of transcriptional regulation requires integration of information obtained from multiple experimental datasets. These include datasets annotating gene expression within the context of an entire organism under normal and genetically perturbed conditions. Here we describe an expression dataset annotating pigment cell-expressed genes of the developing melanocyte and RPE lineages. Expression images are annotated and available at http://research.nhgri.nih.gov/manuscripts/Loftus/March2009/. Data is also summarized in a standardized manner using a universal melanoblast scoring scale that accounts for the embryonic location of cells and regional cell density. This approach allowed us to classify 14 pigment genes into 4 groupings classified by cell lineage expression, temporal-spatial context, and differential alteration in response to altered MITF and SOX10 status. Significant differences in regional populations were also observed across inbred strain backgrounds highlighting the value of this approach to identify modifier allele influences on melanoblast number and distributions. This analysis revealed novel features of *in vivo* expression patterns that are not measurable by *in vitro*-based assays, providing data that in combination with genomic analyses will allow modeling of pigment cell gene expression in development and disease.

Keywords

Melanoblast; Retinal Pigmented Epithelium; *in situ* Hybridization; MITF; SOX10

Introduction

The complete sequencing of the human and mouse genomes has provided the raw material necessary to unravel the regulation of mammalian gene transcription during development. However, we are only beginning to learn to read the genome and understand the language of transcriptional regulation, given the tremendous complexity of factors that govern gene expression. In order to begin to decode the language of gene regulation we need to identify locus-specific, DNA-intrinsic factors, such as chromatin accessibility, methylation status, and primary DNA sequence that reflects the type, number and location of specific protein binding sites (Walhout, 2006). In addition we need to generate experimentally derived data sets of high quality that describe gene expression. These data sets should not only describe

[*]Correspondence to: Stacie K. Loftus, Genetic Disease Research Branch, National Human Genome Research Institute, National Institutes of Health, 49 Convent Dr. MSC4472, Bldg 49/Rm 4A66, Bethesda MD 20892-4472, sloftus@mail.nih.gov, Phone: 301-594-1752, Fax: 301-402-2170.

Supporting Information
Additional Supporting Information may be found in the online version of this article:

gene expression within the context of an isolated cell, but should also detail expression for a single gene across multiple tissues and within the context of an entire organism. An inherent challenge is merging both the experimental data with computational predictions, in a manner that accurately describes all biological observations for a given gene (Elnitski et al., 2006).

Pigment cells are an ideal cell type for developmental transcriptional network analyses because they are readily identified *in vivo*, they express a subset of genes that exhibit very restricted tissue expression, and initial data with respect to the transcriptional hierarchies of these pigment cell-expressed genes has already been collected (Goding, 2000; Hou and Pavan, 2008). Added to this are large datasets that identify locations of specific protein-DNA interactions in pigment cells (Lee et al., 2008; Ozsolak et al., 2007), and datasets generated through the integration of numerous microarray-based gene expression datasets that identify correlations in gene expression between pigment cell transcription factors and potential target genes (Hoek et al., 2006). Such datasets can be used to make predicted transcription factor networks (Hawkins and Ren, 2006). However, in most cases these will require subsequent analysis and experimental validation using *in vivo* models, in order to annotate gene expression for defined tissues/cell types in a manner which will allow for evaluation of computationally-derived, predictive gene expression models. We here outline a systematic methodology applied to generate a gene expression dataset resource that incorporates temporal–spatial expression information and is pigment cell-lineage centric.

During embryonic development, pigment cells arise from two distinct cell lineages, the neural crest and the neural epithelium. Those that are derived from the neural crest, termed melanoblasts during development and melanocytes once differentiated, emigrate from the top of the neural tube and migrate laterally throughout the embryo, subsequently proliferating and migrating throughout the entire embryo until they reach their final destinations of the dermis/hair follicles, inner ear, Harderian gland, and iris and choroid of the eye. Neuroectoderm-derived pigment cells, which form the retinal pigmented epithelium (RPE) layer of the eye, develop from the optic cup, which arises from an out-pocketing of the presumptive forebrain region of the neural tube.

Both pigment cell lineages are characterized by a common set of genes expressed during development, many of which are known to be transcriptional targets of the “master” regulatory factor Microphthalmia-associated Transcription Factor (MITF) (Goding, 2000; Levy et al., 2006; Steingrimsson et al., 2004). *Mitf* mRNA expression is seen in both the developing RPE and the migratory melanoblast cell lineage (Nakayama et al., 1998; Nguyen and Arnheiter, 2000). The neuroectodermal lineage first expresses *Mitf* throughout the optic cup at E9.5, with *Mitf* expression later becoming limited to the developing RPE. *Mitf*-positive melanoblasts are first identifiable near the otocyst at E10.5, displaying a punctate pattern along the lateral sides of the murine embryo at E11.5 (Figure 1). Of note, the roles of MITF in regulating gene expression in the RPE and melanoblasts are similar but not identical (Nakayama et al., 1998).

Currently twenty-nine mutant alleles of *Mitf* have been identified in the mouse. These include both recessive and semi-dominant mutations, and display hypopigmentation that ranges from moderate spotting to complete absence of mature melanocytes (http://www.informatics.jax.org). The *Mitf* mutant allele $Mitf^{mi}$ is semidominant, with heterozygotes displaying reduced iris pigmentation and white spotting on the head, belly and tail, and homozygotes displaying microphthalmia, deafness, and a completely white coat that arise from ocular defects and a complete absence of dermal and stria vascularis melanocytes, respectively(Hodgkinson et al., 1993). Detailed analyses of the effect of the $Mitf^{mi}$ allele on RPE development at E13.5-14.5 have shown that the RPE of $Mitf^{mi/mi}$ embryos begins to develop, however it displays thickening due to cellular hypoproliferation

(as does the RPE of additional *Mitf* mutant mutants) (Nakayama_98). Pigmentation of the RPE is never attained, and subsequently the dorsal RPE transdifferentiates into ectopic neural retina (Nakayama et al., 1998), (Bumsted and Barnstable, 2000). Consistent with this physiological characterization of the $Mitf^{mi/mi}$ eye, E11.5 $Mitf^{mi/+}$ heterozygous embryos have visibly reduced RPE pigmentation and $Mitf^{mi/mi}$ homozygotes a complete lack of RPE pigmentation.

In the melanocyte lineage but not the RPE, *Mitf* itself is directly under the transcriptional regulation of the HMG-box transcription factor SOX10 (Bondurand et al., 2000a; Potterf et al., 2000; Verastegui et al., 2000) and mutations in both *Mitf* and *Sox10* lead to white spotting in mice (Herbarth et al., 1998; Hodgkinson et al., 1993; Hughes et al., 1993; Southard-Smith et al., 1998) and hypopigmentation in human disease (Amiel et al., 1998; Pingault et al., 1998; Tassabehji et al., 1994). *Sox10* is expressed in migratory melanoblasts, the otic vesicle, and sympathetic, enteric, cranial and dorsal root ganglia lineages (Pusch et al., 1998; Southard-Smith et al., 1998). *In situ* hybridization for endogenous *Sox10* expression shows that *Sox10*-positive melanoblasts are first identifiable at E11.5 and that *Sox10* is notably absent from RPE (Britsch et al., 2001; Southard-Smith et al., 1998). In addition to the critical functions that both *Sox10* and *Mitf* perform during embryonic development, their signaling pathways have been implicated in cancer progression for melanoma, as *MITF* is amplified in 10–20% of melanoma metastases (Garraway et al., 2005), and mutations in either *MITF* or *SOX10* have been observed in ~ 20% of melanoma lesions (Cronin et al., 2009). Thus the SOX10-MITF transcriptional pathways in melanocytes regulate genes that are fundamental to the processes of development, differentiation, and cell survival, having implications for disease states of the pigment cell lineage such as melanoma.

We here describe an expression dataset for 14 pigment cell-expressed genes of the developing melanocyte and RPE lineages that are known or putative downstream targets of MITF. We have established this expression data set as a resource to provide a common method of annotation in which to describe the complexities underlying differential gene expression within the context of pigment cell lineages. This methodology can be applied to other genes exhibiting expression in the pigment cell lineages, allowing for standardized description of pigment cell gene expression that will allow for controlled comparison of gene expression for analysis performed in multiple laboratories. Our results reveal novel differences of *in vivo* expression patterns that are not measurable by *in vitro*-based assays. Utilizing this approach, the data obtained from systematic description of gene expression with overlapping yet distinct developmental pigment cell expression patterns will allow the generation of developmental models that will facilitate gene identification and prediction of alterations in disease states such as melanoma.

Results

Gene expression groups defined by pigment cell lineage

Fourteen genes were selected for *in vivo* developmental expression analysis in mouse: *Sox10*, *Mitf*, endothelin receptor type B (*Ednrb*), kit oncogene (*Kit*), dopachrome tautomerase (*Dct*), tyrosinase related protein 1 (*Tyrp1*), tyrosinase (*Tyr*), solute carrier family 45, member 2 (*Slc45a2*), silver (*Si*), glycoprotein (transmembrane) nmb (*Gpnmb*), v-erb-b2 erythroblastic leukemia viral oncogene homolog 3 (avian) (*Erbb3*), melan-A (*Mlana*), transient receptor potential cation channel, subfamily M, member 1 (*Trpm1/Mlsn*) and RAB38, member RAS oncogene family (*Rab38*). These genes were selected because previous studies had shown expression in terminally differentiated melanocyte derived cell lines, that their expression patterns overlapped with those of the transcription factors *Mitf* and *Sox10*, that they were transcriptional targets of SOX10 or MITF when analyzed by *in*

vitro assay systems, and/or that they exhibited reduced expression in mouse models harboring mutations of *Sox10* and *Mitf* (Baxter and Pavan, 2002; Baxter and Pavan, 2003; Bentley et al., 1994; Britsch et al., 2001; Du and Fisher, 2002; Du et al., 2003; Hou et al., 2006; Keshet et al., 1991; Loftus et al., 2008; Loftus et al., 2002; Miller et al., 2004; Murisier et al., 2007; Sato-Jin et al., 2008; Steel et al., 1992; Tsujimura et al., 1996; Yasumoto et al., 1997). However, as multiple laboratories performed these studies at different stages of embryonic development and on different or undefined genetic backgrounds, it was difficult to develop models by direct comparisons among the reported gene expression patterns.

To enable a controlled comparison of gene expression patterns for this 14-gene set, we performed whole mount *in situ* hybridization for each gene at E11.5 on a C57BL/6J background (Supplemental Table 1). The developmental time point of E11.5 was selected as it captures the first time point when melanoblasts, prior to differentiation and melanin production, are actively migrating throughout the entire length of the embryo. Comparison of the gene expression patterns allowed grouping of the genes into lineage based categories as follows: Class 1: melanoblasts +, RPE + (*Tyr, Dct, Gpnmb, Mitf, Slc45a2, Si*); Class II: melanoblasts +, RPE − (*Kit, Ednrb, Sox10, Erbb3*), and Class III: melanoblasts -, RPE + (*Mlsn, Tyrp1, Rab38, Mlana*). The genes represented in Class II are then further stratified with respect to PNS expression: Class IIa: melanoblasts +, RPE −, PNS− (*Kit*), and Class IIb: melanoblasts +, RPE −, PNS+ (*Ednrb, Sox10, Erbb3)*(Figure 1). The scoring for each of the genes to be present or absent in early melanoblasts was based on the following criteria: (i) Replicable pattern of punctate, isolated cell populations; (ii) The location of the isolated cells occurs in regions consistent with the location of LacZ positive cells from *tgDct*-lacZ mice (Mackenzie et al., 1997); (iii) The expression is absent in these regions in melanoblast-deficient $Mitf^{mi/mi}$ embryos (detailed below).

Visual documentation of comprehensive melanoblast gene expression over an entire embryo can be difficult to capture in a single image, given that melanoblasts are small, independent cells found dispersed across multiple focal planes of a three-dimensional E11.5 embryo. Thus we have created a web accessible database (Supplemental Figure S1) with multiple images capturing the gene expression in the head, otic vesicle, trunk and tail regions independently, in addition to the a side views of embryos representing the whole mount *in situ* performed for the 14 genes, located at http://research.nhgri.nih.gov/manuscripts/Loftus/March2009/.

Regional Melanoblast Density Scale

To summarize the image results and to represent the variation observed for the melanoblast *in situ* patterns in a standardized manner, we created a melanoblast scoring scale. This approach analyzes the gene expression pattern, and incorporates both the embryonic spatial location and the regional density of cells expressing a given gene. The embryo was divided into eight regions, and a 0–4 melanoblast density scale (MDS) score was used to assign a quantitative value to the density of melanoblasts expressing a given gene in each region (Figure 2). Individuals who were blinded to embryo genotype scored the left and right sides of each embryo independently. Scores were then averaged and converted to a MDS heatmap to facilitate summary and comparison (Figure 3). Of note, the MDS describes the observable melanoblast cell populations that can be detected by *in situ* hybridzation for a given gene. The MDS scoring is not based on whether the individual melanoblast cells observed were of lower or higher intensity, which might be affected by a number of factors including: variations in the expression level of a given gene, variations in hybridization due to probe sequences and/or variation of signal generation in the defined detection conditions.

C57BL/6J melanoblast density and distribution

For each of the eight embryonic regions defined at E11.5, we then compared the MDS scores for the lineage-defined Class I genes (*Tyr, Dct, Gpnmb, Mitf, Slc45a2, and Si*) and Class IIa gene (*Kit*) in E11.5 C57BL/6J embryos. We observed that MDS scores for multiple genes captured a similar trend in spatial melanoblast distribution across the embryo despite variation among these seven genes in the *in situ* signal intensity per melanoblast. For each of these genes the consistent trend was as follows: the highest MDS scores were found over the otocyst (region D) and at the area of the hind limb and distal to the tail (regions G and H respectively), while a reduced MDS score was consistently observed in the area of the fore limb (region E) and in the area of the trunk between the limbs (region F) (Figure 3, Supplemental Figure S2).

Melanoblast density varies among inbred strains

Given the known variation that occurs among inbred mouse strains with respect to variability in white spotting (Asher et al., 1996; Britsch et al., 2001; Pavan et al., 1995; Southard-Smith et al., 1999), we hypothesized that MDS scores may vary depending on allelic polymorphisms of genes segregating across the genetic background of the embryo analyzed. To test this, we performed standardized *in situ* hybridization of *Si* on E11.5 embryos of six inbred strains (C57BL/6J, DBA/2J, BALB/cJ, FVB/NJ, C3H/HeJ, and 129SvEv/Tac) (Supplemental Figure S3) and image results were summarized using the MDS (Figure 4, Table 1). The resulting *in vivo* expression patterns of *Si*-positive melanoblasts at E11.5 varied in a region-independent, yet strain-specific manner with several significant variations of MDS scores (Supplemental Table 2). For example, in FVB/NJ the embryos exhibited a uniform, dense population of melanoblasts across the trunk region (region F), which differed significantly ($p < 0.001$) from the sparse population of cells in this region observed in C57BL/6J and C3H/HeJ. However, when the melanoblast cell density in the rostral head (region A) was evaluated (figure 4A, B), it was the strains FVB/NJ, DBA/2J and C3H/HeJ that exhibited a reduction in cell density compared to the dense expression pattern observed in BALB/cJ ($p < 0.001$). Finally, analysis of 129SvEv/Tac embryos demonstrated a significant reduction in the number of melanoblasts in the distal tail (region H) in comparison to the strains C57BL/6J, DBA/2J, BALB/cJ, and FVB/NJ ($p < 0.001$). Expanding this approach to other inbred strains and specific crosses may allow the identification of polymorphic loci that may account for these differences.

Mitf and *Sox10* effects on melanoblast gene expression patterns

In addition to variation of MDS score due to strain polymorphisms, we wanted to evaluate how the expression of early melanoblast marker genes is affected by variation in individual gene expression. Our initial analysis focused on embryos with functional variation in the transcription factors *Sox10* or *Mitf*. Given the influence we observed of genetic background on MDS scoring, we used mice that were congenic for $Sox10^{tm1Weg}$ and $Mitf^{mi}$ on a C57BL/6J background. Gene expression patterns were evaluated for stage-matched, E11.5 littermates that were either wild type, heterozygous or homozygous for $Sox10^{tm1Weg}$ or $Mitf^{mi}$. To facilitate visulization, the data is summarized using two MDS heatmaps: one sorted by embryo genotype (Figure 3) and one sorted by gene probe (Supplemental Figure S4).

Formatting of the summarized *in situ* data in this manner allowed comparisons across multiple genes and genotypes for the dataset, and revealed differences with respect to how distinct melanoblast populations and individual genes responded to alterations in *Mitf* and *Sox10* levels. For example, evaluation of the genotype-sorted data (Figure 3) identified a unique population of *Mitf*-expressing melanoblasts present in both the homozygous $Mitf^{mi/mi}$ and $Sox10^{tm1Weg/tm1Weg}$ mice within the dorsal tail. Of the six other melanoblast-expressed

Mitf target genes, only *Gpnmb* is also found expressed within this discrete population in *Sox10*$^{tm1Weg/tm1Weg}$ embryos; with no *Gpnmb* expression seen in these cells in *Mitf* $^{mi/mi}$ embryos.

Evaluation of the MDS dataset as a whole also allowed us to further characterize and subdivide the group of six Class I genes. Although all six genes in Class I present with a similar reduction in gene-positive melanoblast numbers is observed in *Mitf*$^{mi/+}$embryos relative to wild-type, this is not what is observed for the same set of genes evaluated in context of *Sox10*$^{tm1Weg/+}$ embryos. In *Sox10*$^{tm1Weg/+}$ embryos, *Mitf*, *Slc45A2* and *Tyr* exhibited a visible reduction in melanoblast numbers relative to wild-type C57BL/6J embryos, however this reduction is comparable to that which is also observed in *Mitf*$^{mi/+}$embryos. However for *Dct*, the number of *Dct*-positive melanoblasts observed is in *Sox10*$^{tm1Weg/+}$ embryos is less than the number of *Dct*+ melanoblasts obeserved in *Mitf*$^{mi/+}$embryos and fewer than what is seen for the other Class I genes in *Sox10*$^{tm1Weg/+}$ embryos. Distinct from both of the previous examples is the regulation of gene expression for both *Gpmnb* and *Si*. For *Gpmnb* and *Si*, the number of gene-positive melanoblasts observed in *Sox10*$^{tm1Weg/+}$ embryos was higher than that observed for *Dct*, *Slc45A2* and *Tyr*. For the Class IIa gene *Kit*, analysis of the MDS dataset further defines how transcriptional regulation of *Kit* is distinct from the group of the Class I genes. *Kit* is the sole gene to remain expressed in a population of punctate cells that is present along the entirety of the *Mitf*$^{mi/mi}$ embryos, while only a small, discrete number of *Kit* + cells could be observed over the hindlimb area in *Sox10*$^{tm1Weg/tm1Weg}$ embryos.

Effect of *Mitf* on RPE gene expression

Although the RPE and melanoblasts are derived from distinct tissues, both are pigmented cell types in which MITF has been shown to play a fundamental role regulating gene expression. Therefore, we examined the effect of altered *Mitf* expression on the gene expression patterns for the ten Class I and Class III genes that were expressed in the RPE (Figure 5). When the RPE gene expression patterns were grouped based upon expression levels in wildtype, *Mitf*$^{mi/+}$ and *Mitf*$^{mi/mi}$ embryos at E11.5, five distinct patterns of RPE expression were observed (Figure 5b). The RPE Group 1 genes, *Mitf*, *Rab38*, and *Trpm1*, remain expressed in the RPE even within the context of a reduction in functional MITF in *Mitf*$^{mi/+}$and *Mitf*$^{mi/mi}$ embryos. Notably, the *in situ* hybridization signal for *Mitf* mRNA itself in the *Mitf*$^{mi/mi}$ RPE appeared more intense, although this may reflect the cellular hypoproliferation previously observed in the *Mitf*$^{mi/mi}$ RPE (Nakayama et al., 1998). This is distinct from the RPE Group 2, consisting solely of *Dct*, in which RPE expression is maintained in *Mitf*$^{mi/mi}$ embryos, although at diminished levels. This is consistent with previous *Dct in situ* analysis (Nakayama et al., 1998). The remaining six genes are not expressed in the RPE of *Mitf*$^{mi/mi}$ embryos, however their corresponding expression patterns can be further subdivided into three additional groupings. RPE Group 3 genes, consisting of *Slc45a2* and *Tyr*, are expressed in the RPE in *Mitf*$^{mi/+}$ and wildtype in a similar manner; RPE Group 4 genes, consisting of *Gpnmb*, *Mlana*, and *Si*, show decreased probe intensity in the RPE in *Mitf*$^{mi/+}$ embryos compared to wildtype; and RPE Group 5, consisting solely of *Tyrp1*, shows no RPE expression in *Mitf*$^{mi/+}$embryos. In summary, using a controlled scoring system on defined inbred and genetic backgrounds, we have been able to subdivide 14 pigment cell expressed genes into distinct classes and groupings. This approach and data is an important step towards fully developed models describing the network of gene regulation in melanocytes and understanding how they are perturbed in disease states.

Discussion

Comprehensive gene expression data can provide a powerful resource for predicting and building models of gene regulatory networks. Identifying all the factors that control where,

when and to what level mRNA is produced will be essential for deciphering the common language governing transcriptional regulation. Work is being done to indentify sequence elements that convey lineage, spatial and temporal expression information for a gene. However an integral part of such analyzes will be datasets containing the *in vivo*, temporal-spatial descriptions of gene expression in experimentally manipulated environments. We have focused on developing a method to reproducibly characterize gene expression in pigment cell lineages at E11.5 in the mouse. This captures a time when early melanoblasts are present along the entirety of the embryo and are undergoing active migration and proliferation. It is within this context that we have generated a pigment cell gene expression dataset, using systematic evaluation criteria to identify distinct melanoblast populations and categorize genes based on *in situ* gene expression.

An inherent requirement of using whole mount *in situ* hybridization data for comparative analyses is appropriate quantitation and spatial annotation of the data. To accomplish this, we have developed a defined MDS scoring system tailored to the melanoblast lineage, to rapidly, systematically and reproducibly annotate the melanoblast gene expression pattern. This system can be applied to multiple embryos and used to compare genes within backgrounds or genes in the context of genetic or environmental variations. It is important to note that the MDS system is a quantitative score of melanoblast number based on *in situ* hybridization detection of a specific gene. Thus if the *in situ* hybridization signal for a gene is detectible in all melanoblasts, than the MDS score is reflective of the total melanoblast number present in a given embryonic region. Alternatively, the MDS score may represent a sub-population of melanoblasts for several reasons. For example systemic perturbation (such as genetic background or inclusion of a genetic mutation) or natural variation of gene expression may result in a subset of melanoblasts with undetectable levels of the gene without affecting overall melanoblast cell numbers. Both indices are biologically important to identify, however one must be mindful of these parameters when incorporating appropriate controls and interpreting the data using this approach.

With this *in situ* data set we find examples where the MDS score captures either gene expression differences, or a reduction in overall melanoblast numbers in the embryo. An Examples of our ability to capture gene expression differences is found from the comparative analysis of all Class I genes in transcription factor-haploinsufficient conditions. Here analysis of *Dct* expression revealed a significant reduction in the number of *Dct* + melanoblasts found in $Sox10^{tm1Weg/+}$ embryos in comparison to $Mitf^{mi/+}$embryos. None of the other Class 1 genes exhibits a similar reduction in gene+ melanoblasts in $Sox10^{tm1Weg/+}$ embryos. Taken together these results indicate that there are more melanoblasts present in $Sox10^{tm1Weg/+}$ embryos than are found to be *Dct*+, and that an *in vivo* reduction in SOX10 levels results in a more dramatic reduction in *Dct* expression than observed due to alteration in MITF levels alone. These *in vivo* results are consistent with what we have observed through *in vitro* promoter transactivation assays indicating that both SOX10 and MITF synergistically regulate *Dct* expression (Jiao et al., 2004; Ludwig et al., 2004; Potterf et al., 2001), and that *Mitf* is also a direct target of SOX10 (Potterf et al., 2000), (Bondurand et al., 2000b) and would thus be reduced in $Sox10^{tm1Weg/+}$ embryos(Britsch et al., 2001). These results also suggest that unlike *Dct*, the promoters for the genes *Si, Gpnmb, Slc45A2 and Tyr* would not be predicted to respond to MITF and SOX10 in a synergistic manner.

Another example of the capacity of the MDS score to capture variation in gene expression levels is observed for analysis of *Gpnmb* and *Si*. We observed that for both genes *Gpnmb* and *Si* there were more gene-positive melanoblasts across the entirety of the embryo in $Sox10^{tm1Weg/+}$ embryos than in $Mitf^{mi/+}$ embryos. Given that three other melanoblast genes, *Mitf, Slc45a2* and *Tyr* present with similar numbers of melanoblasts in both *Sox10* and *Mitf* heterozygous mice we suggest that regulatory elements governing *Si* and *Gpnmb* gene

expression may be more sensitive to reductions in functional MITF levels than to reductions in SOX10. Therefore *Gpnmb* and *Si* can be grouped distinctly from the other Class I genes, *Dct*, *Slc45a2* and *Tyr*. Future systematic analysis of the cis-regulatory regions of these genes correlated with annotation of the melanoblast and RPE lineage repertoire of available transcription factors at E11.5 will be required in order to begin to make more comprehensive predictive models that define these gene expression patterns.

The MDS score also captures gene expression differences with respect to location of gene-positive cell populations *in vivo*. For example, *Mitf* and *Gpnmb* gene expression patterns are distinct relative to the other genes in this data set when comparing the MDS heatmap profiles in $Mitf^{mi/mi}$ and $Sox10^{tm1Weg/tm1Weg}$ homozygous embryos. Previously, we observed *Gpnmb*- and *Mitf*-positive cells marking *Sox10*-independent melanoblasts in a discrete region over the hind limb and tail at E11.5 (Loftus et al., 2008). Here we have extended the analysis of this population of cells in $Sox10^{tm1Weg/tm1Weg}$ embryos, and determined that *Dct*, *Si*, *Tyr*, and *Slc45a2* are not expressed in this newly defined cell population. Possibly this distinct gene expression pattern may be correlated with the observation that *Gpnmb* is also found to be regulated by MITF in the osteoclast cell lineage (Ripoll et al., 2008). Future analyses will be required to determine precisely what factors are contributing to the SOX10-independent expression of these two genes in the caudal melanoblast population and thus differentiate *Mitf* and *Gpnmb* from other pigment cell expressed genes.

Analysis of our dataset also provides examples of how genes can be categorized based on temporal-spatial and lineage information. For example, if expression were only examined in terminally differentiated melanocyte cell populations, most genes in this study would be grouped into one Class. However analysis at E11.5 showed that *Gpnmb, Si, Slc45a2*, *Dct* and *Tyr* (Class I) can be distinguished from *Trpm1, Mlana*, and *Tyrp1* (Class II), as the latter are not expressed in melanoblasts at the E11.5 timepoint (Figure 1). This temporal difference is not due to whether or not Class III genes are MITF targets genes, as experimental evidence demonstrates that MITF contributes to the regulation of *Trpm1, Mlana*, and *Tyrp1* in pigmented melanocytes and melanoma cells (Du et al., 2003;Yasumoto et al., 1995;Zhiqi et al., 2004). This data suggests that a more complex interaction of regulatory factors, in combination with MITF, regulate the temporal initiation of gene expression in early melanoblasts versus melanocytes.

Finally, by applying the MDS scoring system to comparison of multiple inbred strains, we demonstrate that early in melanoblast development, patterns can vary significantly depending on the strain background and embryonic location. In this case the variation observed is likely not due to modifier loci merely reducing *Si* expression in a region specific manner, as we have observed greater numbers of trunk melanoblasts in E11.5 FVB/NJ mice than in C56BL/6J mice for *Dct*, *Gpnmb*, and *Slc45A2* expression (Baxter and Pavan, 2003), and unpublished data), similar to what is seen for *Si* in these two strains. Thus the strain dependant variation in numbers of *Si*-positive melanoblasts is likely due to regional differences in melanoblast numbers between strains and not due to variations in levels of *Si* gene expression within melanoblasts. Taken together this suggests that there are strain-dependant modifiers of early melanoblast numbers in the embryo. It has long been appreciated that the location and size of hypo-pigmented areas in adult mice are inherited as quantitative traits (Doolittle et al., 1975; Dunn and Charles, 1937; Pavan et al., 1995) and it has more recently been demonstrated that the background strains onto which the spotting mutation alleles *Ednrb*, *Pax3* and *Sox10* are maintained affect the severity of the spot (Asher et al., 1996; Britsch et al., 2001; Pavan et al., 1995; Southard-Smith et al., 1999). However, the total number of loci that represent strain-specific modifiers of hypopigmentation remains to be determined. Currently, 104 genes and/or loci are annotated in the MGI database that exhibit some degree of “white spotting” (http://www.informatics.jax.org/), with typical

patterns being belly spots, head spots, piebald spotting, and white “belts” which encircle the caudal trunk (Baxter et al., 2004). These genes/loci are known to affect a variety of melanoblast/melanocyte cellular processes including migration, differentiation proliferation, and cell survival. There is the potential for numerous pigmentation modifier loci to segregate among the many inbred strains. Application of the MDS scoring system in the context of a consistent inbred strain background can verify that the details of gene expression differences such as those described here can be correctly attributed to either gene-intrinsic variations or independent modifiers.

All 14 genes in this data set are expressed in the terminally differentiated melanocyte lineage, with 8 of 14 genes (*Si, Dct, Gpnmb, Slc45A2, Mlana Tyr, Tyrp1*, and *Trpm1)* classified as MITF transcriptional targets. However, we here demonstrate that not all these genes respond to alteration in MITF levels in a similar manner. Through systematic evaluation of this expression dataset we have been able to sub-divide this gene set into smaller, expression-based, phenotype-correlated gene groupings. These results reinforce the fact that transcriptional regulation is a complex process. Often transcriptional regulation is approached in a simplified manner through the prism of data collected in a single isolated cell type, such as a melanocyte or melanoma derived cell line, under a single condition. Such analysis by default excludes a spatio-temporal based analysis such as observations of marked cell populations during embryonic development. Our dataset and methodology for annotation provides a framework for phenotypic correlations to be made for genes based upon *in vivo* expression characteristics. In the future, in depth functional analysis of genomic elements will be required to obtain detailed and precise gene expression information. More lineage-appropriate gene expression information is required and must be collected in a standardized manner if one is to develop computational models that identify parameters that define where, when, and at what level a gene is expressed. Fundamental to this type of modeling/analysis is information regarding how modulation of a single regulatory expression pathway or a single transcription factor will vary the expression of individual genes and how that variation compares when a collection of genes with defined similar patterns of expression are compared. Cataloging this variation is the first step in identifying temporal-spatial gene expression pattern correlations between genes and regulatory sequence for those genes. These correlations will provide the foundation to annotate and query the common and distinct cis-regulatory factors for each of these genes and will allow for future testing and evaluation of candidate regulatory elements, among additional genes demonstrating similar defined expression patterns, to assess the extent to which these elements are predictive of the expression patterns observed.

Materials and Methods

Mice breeding and genotyping

Mitf$^{Mi/+}$ mice were obtained from Jackson laboratories B6C3 Fe a/a -Mitf/J strain #001573 and backcrossed to C57BL/6J mice for over 15 generations. *Sox10*^{tm1Weg} mice were obtained from Dr. Michael Wegner and backcrossed to C57BL/6J for over 10 generations. Both *Sox10*^{tm1Weg}/+ X *Sox10*^{tm1Weg} and *Mitf*$^{Mi/+}$ X *Mitf*$^{Mi/+}$ mating crosses were setup, corresponding plugs were identified in the morning and established as day E 0.5. At E11.5, embryos were dissected and all embryos were developmentally staged matched based upon limb, eye and craniofacial structures as defined as E11.5 in Kaufmann (Kaufman, 2005). Genotyping of embryos was performed on DNA isolated from corresponding yolk sacs using the PureGene Kit (Gentra Systems, Inc. Minneapolis, MN). *Sox10* genotyping was performed as described (Britsch et al., 2001). *Mitf* genotyping was performed as described (Loftus et al., 2008).

In situ Hybridization

For *in situ* probe generation a summarized list of plasmid cDNA clones, with corresponding appropriate restriction enzyme digests and RNA polymerases that were used is provided in Supplemental Table 1. *In situ* hybridization probes were prepared as indicated previously for the genes *Sox10* (Southard-Smith et al., 1998), *Rab38* (Loftus et al., 2002), *Kit* (Keshet et al., 1991) *Dct* (Steel et al., 1992), and *Ednrb* (Opdecamp et al., 1998). For the following genes, probes were prepared by linearizing the indicated plasmid clone with *KpnI*, followed by reverse transcribing digoxigen-conjugated probes using T3 RNA polymerase (reagents from Roche Molecular Biochemical Mannheim, Germany): *Mitf*, Riken clone #G370008D06; Si, Riken clone #G370069C13; *Gpnmb*, Riken clone #G370004B14; *Mlana*, Riken clone #G370004L04; Slc45a2, Riken clone #G3B70045L22; *Trpm1*, Riken clone #G370028M02; *Tyr*, Riken clone #4633402C07. For *Tyrp1*, EST clone Riken clone #4732408D14 was used as a template for amplification using PCR Primers, TYRP1-5′_T3-F-GCGCGAATTAACCCTCACTAAAGGGTCTGAGCACCCCTGTCTTCT and TYRP1-5_T7-R-GCGCGTAATACGACTCACTATAGGGCCCAGTTGCAAAATTCCAGT) (Loftus et al., 2002). The resulting amplification product was purified using Microcon 100 column (Millipore, Bedford MA) and reverse transcribed using T7 RNA polymerase. For *Erbb3*, plasmid cDNA (gift of Dr. Lidia Kos) was digested with EcoRI and T7 RNA polymerase was used. Whole mount *in situ* hybridization was performed as previously described (Wilkinson and M. A. Nieto, 1993) with these modifications. Ribonuclease A digestion was omitted, and Tris-buffered saline was used in place of PBS. BM-purple substrate (Roche, Molecular Biochemicals) was used in place of 5-bromo-4-chloro-3-indolylphosphate nitroblue tetrazolium. *In situ* hybridizations were performed for each gene probe in the following manner to allow for comparisons between strains and genotypes. For comparison of Si-positive melanoblast expression patterns in the six wild-type inbred strains, four embryos of each strain were processed simultaneously, utilizing identical probe amount, and time of alkaline phosphatase reaction. For comparisons of the gene expression patterns for multiple genes in wild-type C57BL/6J embryos the following numbers of embryos were analyzed: four embryos (*Si*) and three embryos (*Dct*,) and two embryos (*Gpnmb, Kit, Slc45A2, and Tyr*). For comparisons of gene expression in *Sox10* and *Mitf* deficient mice, two embryos of each genotype were hybridized and scored; and for each probe, hybridizations for all 5 genotype conditions were processed simultaneously, utilizing identical probe amount, and time of alkaline phosphatase reaction.

Imaging system

A Leica MZ APO microscope onto which a 3CCD MTI camera (Dage-**MTI**, Michigan City, IN, USA) was attached was used to capture embryo images using Adobe Photoshop 7 and Scion Image 1.63 software.

Melanoblast Density Scale

Region A: defines the melanoblasts found in the crease between the telencephalon and nasal process, extending towards the eye. Region B: defines the melanoblast population found at the crease defining the midbrain, hindbrain boundary. Region C: the area between the caudal boundary line from the eye to the mid-hindbrain in region B and a parallel line immediately anterior to the otic vesicle. Region D: defines the melanoblast population overlying the otic vesicle and extending distal to encompass the melanoblasts migrating across the area corresponding to region overlying cranial ganglia IX and X. Region E: melanoblast population lateral to the forelimb area between areas defined by region D and F. Region F: the melanoblasts present in the trunk as defined by the post axial, (caudal) side of the forelimb bud, throughout the trunk, up to the preaxial (anterior) side of the hindlimb bud.

Region G: melanoblasts immediately lateral to the hind limb area. Region H: the melanoblast population caudal to the post axial hindlimb.

Inbred Strain MDS statistical analysis

A nonparametric ANOVA (Kruskal-Wallis) was used to compare median values across inbred strains in each region (A-H) using commercially available software (InStat, GraphPad Software). All regions failed the null hypothesis at a 95% confidence level and a multiple comparison post-test was used to identify pairs of strains with significant differences in MDS score.

Significance

Identification of the components that delineate spatial and temporal expression for a gene throughout an organism's lifetime is needed to understand gene regulation in both normal and disease settings. Here we generated the framework for a publicly available gene expression dataset for pigment cell genes and have developed a system to compare data across experimental conditions. We focused on gene expression in the eye and melanoblast lineage at mid-gestation in the mouse embryo, when melanoblasts are actively migrating and proliferating. Using systematic evaluation criteria, genes were subdivided based upon their expression patterns in distinct melanoblast populations that vary in time, space and genetic influence. In conjunction with genomic sequence information, this type of comprehensive, *in vivo* gene expression data can provide a powerful resource for building gene regulatory network models.

Supplementary Material

Refer to Web version on PubMed Central for supplementary material.

Acknowledgments

This work was funded through the NIH intramural program, NHGRI. Experiments were performed in accordance with the NHGRI animal care and use protocol G-94-7. We would like to thank Dr. Lidia Kos for *Erbb3* cDNA, Lowell Umayam and Anh-Dao Nguyen (NHGRI Bioinfomatics core) for database design and support, and Darryl Leja (NHGRI) for graphics assistance.

References

Amiel J, Watkin PM, Tassabehji M, Read AP, Winter RM. Mutation of the MITF gene in albinism-deafness syndrome (Tietz syndrome). Clin Dysmorphol. 1998; 7:17–20. [PubMed: 9546825]

Asher JH Jr, Harrison RW, Morell R, Carey ML, Friedman TB. Effects of Pax3 modifier genes on craniofacial morphology, pigmentation, and viability: a murine model of Waardenburg syndrome variation. Genomics. 1996; 34:285–298. [PubMed: 8786127]

Baxter LL, Hou L, Loftus SK, Pavan WJ. Spotlight on spotted mice: a review of white spotting mouse mutants and associated human pigmentation disorders. Pigment Cell Res. 2004; 17:215–224. [PubMed: 15140066]

Baxter LL, Pavan WJ. The oculocutaneous albinism type IV gene Matp is a new marker of pigment cell precursors during mouse embryonic development. Mech Dev. 2002; 116:209–212. [PubMed: 12128226]

Baxter LL, Pavan WJ. Pmel17 expression is Mitf-dependent and reveals cranial melanoblast migration during murine development. Gene Expr Patterns. 2003; 3:703–707. [PubMed: 14643677]

Bentley NJ, Eisen T, Goding CR. Melanocyte-specific expression of the human tyrosinase promoter: activation by the microphthalmia gene product and role of the initiator. Mol Cell Biol. 1994; 14:7996–8006. [PubMed: 7969139]

Bondurand N, Pingault V, Goerich DE, Lemort N, Sock E, Caignec CL, Wegner M, Goossens M. Interaction among SOX10, PAX3 and MITF, three genes altered in Waardenburg syndrome. Hum Mol Genet. 2000a; 9:1907–1917. [PubMed: 10942418]

Bondurand N, Pingault V, Goerich DE, Lemort N, Sock E, Le Caignec C, Wegner M, Goossens M. Interaction among SOX10, PAX3 and MITF, three genes altered in Waardenburg syndrome. Hum Mol Genet. 2000b; 9:1907–1917. [PubMed: 10942418]

Britsch S, Goerich DE, Riethmacher D, Peirano RI, Rossner M, Nave KA, Birchmeier C, Wegner M. The transcription factor Sox10 is a key regulator of peripheral glial development. Genes Dev. 2001; 15:66–78. [PubMed: 11156606]

Bumsted KM, Barnstable CJ. Dorsal retinal pigment epithelium differentiates as neural retina in the microphthalmia (mi/mi) mouse. Invest Ophthalmol Vis Sci. 2000; 41:903–908. [PubMed: 10711712]

Cronin JC, Wunderlich J, Loftus SK, Prickett TD, Wei X, Ridd K, Vemula S, Burrell AS, Agrawal NS, Lin JC, et al. Frequent Mutations in the MITF Pathway in Melanoma. Pigment Cell Melanoma Res. 2009

Doolittle DP, Wilson SP, Hulbert LL, Kyle WH, Goodale HD. The Goodale white-spotted mice: a historical report. J Hered. 1975; 66:376–380. [PubMed: 767403]

Du J, Fisher DE. Identification of Aim-1 as the underwhite mouse mutant and its transcriptional regulation by MITF. J Biol Chem. 2002; 277:402–406. [PubMed: 11700328]

Du J, Miller AJ, Widlund HR, Horstmann MA, Ramaswamy S, Fisher DE. MLANA/MART1 and SILV/PMEL17/GP100 are transcriptionally regulated by MITF in melanocytes and melanoma. Am J Pathol. 2003; 163:333–343. [PubMed: 12819038]

Dunn LC, Charles DR. Studies on Spotting Patterns I. Analysis of Quantitative Variations in the Pied Spotting of the House Mouse. Genetics. 1937; 22:14–42. [PubMed: 17246828]

Elnitski L, Jin VX, Farnham PJ, Jones SJ. Locating mammalian transcription factor binding sites: a survey of computational and experimental techniques. Genome Res. 2006; 16:1455–1464. [PubMed: 17053094]

Garraway LA, Widlund HR, Rubin MA, Getz G, Berger AJ, Ramaswamy S, Beroukhim R, Milner DA, Granter SR, Du J, et al. Integrative genomic analyses identify MITF as a lineage survival oncogene amplified in malignant melanoma. Nature. 2005; 436:117–122. [PubMed: 16001072]

Goding CR. Mitf from neural crest to melanoma: signal transduction and transcription in the melanocyte lineage. Genes Dev. 2000; 14:1712–1728. [PubMed: 10898786]

Hawkins RD, Ren B. Genome-wide location analysis: insights on transcriptional regulation. Hum Mol Genet. 2006; 15(Spec No 1):R1–7. [PubMed: 16651365]

Herbarth B, Pingault V, Bondurand N, Kuhlbrodt K, Hermans-Borgmeyer I, Puliti A, Lemort N, Goossens M, Wegner M. Mutation of the Sry-related Sox10 gene in Dominant megacolon, a mouse model for human Hirschsprung disease. Proc Natl Acad Sci U S A. 1998; 95:5161–5165. [PubMed: 9560246]

Hodgkinson CA, Moore KJ, Nakayama A, Steingrimsson E, Copeland NG, Jenkins NA, Arnheiter H. Mutations at the mouse microphthalmia locus are associated with defects in a gene encoding a novel basic-helix-loop-helix-zipper protein. Cell. 1993; 74:395–404. [PubMed: 8343963]

Hoek KS, Schlegel NC, Brafford P, Sucker A, Ugurel S, Kumar R, Weber BL, Nathanson KL, Phillips DJ, Herlyn M, et al. Metastatic potential of melanomas defined by specific gene expression profiles with no BRAF signature. Pigment Cell Res. 2006; 19:290–302. [PubMed: 16827748]

Hou L, Arnheiter H, Pavan WJ. Interspecies difference in the regulation of melanocyte development by SOX10 and MITF. Proc Natl Acad Sci U S A. 2006; 103:9081–9085. [PubMed: 16757562]

Hou L, Pavan WJ. Transcriptional and signaling regulation in neural crest stem cell-derived melanocyte development: do all roads lead to Mitf? Cell Res. 2008; 18:1163–1176. [PubMed: 19002157]

Hughes MJ, Lingrel JB, Krakowsky JM, Anderson KP. A helix-loop-helix transcription factor-like gene is located at the mi locus. J Biol Chem. 1993; 268:20687–20690. [PubMed: 8407885]

Jiao Z, Mollaaghababa R, Pavan WJ, Antonellis A, Green ED, Hornyak TJ. Direct interaction of Sox10 with the promoter of murine Dopachrome Tautomerase (Dct) and synergistic activation of Dct expression with Mitf. Pigment Cell Res. 2004; 17:352–362. [PubMed: 15250937]

Kaufman, MW. Atlas of Mouse Development. Amsterdam: Elsevier Academic Press; 2005.

Keshet E, Lyman SD, Williams DE, Anderson DM, Jenkins NA, Copeland NG, Parada LF. Embryonic RNA expression patterns of the c-kit receptor and its cognate ligand suggest multiple functional roles in mouse development. EMBO J. 1991; 10:2425–2435. [PubMed: 1714375]

Lee KE, Nam S, Cho EA, Seong I, Limb JK, Lee S, Kim J. Identification of direct regulatory targets of the transcription factor Sox10 based on function and conservation. BMC Genomics. 2008; 9:408. [PubMed: 18786246]

Levy C, Khaled M, Fisher DE. MITF: master regulator of melanocyte development and melanoma oncogene. Trends in molecular medicine. 2006; 12:406–414. [PubMed: 16899407]

Loftus SK, Antonellis A, Matera I, Renaud G, Baxter LL, Reid D, Wolfsberg TG, Chen Y, Wang C, Prasad MK, et al. Gpnmb is a Melanoblast-Expressed, MITF-Dependent Gene. Pigment Cell Melanoma Res. 2008

Loftus SK, Larson DM, Baxter LL, Antonellis A, Chen Y, Wu X, Jiang Y, Bittner M, Hammer JA, Pavan WJ. Mutation of melanosome protein RAB38 in chocolate mice. Proc Natl Acad Sci USA. 2002; 99:4471–4476. [PubMed: 11917121]

Ludwig A, Rehberg S, Wegner M. Melanocyte-specific expression of dopachrome tautomerase is dependent on synergistic gene activation by the Sox10 and Mitf transcription factors. FEBS Lett. 2004; 556:236–244. [PubMed: 14706856]

Mackenzie MA, Jordan SA, Budd PS, Jackson IJ. Activation of the receptor tyrosine kinase Kit is required for the proliferation of melanoblasts in the mouse embryo. Dev Biol. 1997; 192:99–107. [PubMed: 9405100]

Miller AJ, Du J, Rowan S, Hershey CL, Widlund HR, Fisher DE. Transcriptional regulation of the melanoma prognostic marker melastatin (TRPM1) by MITF in melanocytes and melanoma. Cancer Res. 2004; 64:509–516. [PubMed: 14744763]

Murisier F, Guichard S, Beermann F. The tyrosinase enhancer is activated by Sox10 and Mitf in mouse melanocytes. Pigment Cell Res. 2007; 20:173–184. [PubMed: 17516925]

Nakayama A, Nguyen MT, Chen CC, Opdecamp K, Hodgkinson CA, Arnheiter H. Mutations in microphthalmia, the mouse homolog of the human deafness gene MITF, affect neuroepithelial and neural crest-derived melanocytes differently. Mech Dev. 1998; 70:155–166. [PubMed: 9510032]

Nguyen M, Arnheiter H. Signaling and transcriptional regulation in early mammalian eye development: a link between FGF and MITF. Development. 2000; 127:3581–3591. [PubMed: 10903182]

Opdecamp K, Kos L, Arnheiter H, Pavan WJ. Endothelin signalling in the development of neural crest-derived melanocytes. Biochem Cell Biol. 1998; 76:1093–1099. [PubMed: 10392719]

Ozsolak F, Song JS, Liu XS, Fisher DE. High-throughput mapping of the chromatin structure of human promoters. Nat Biotechnol. 2007; 25:244–248. [PubMed: 17220878]

Pavan WJ, Mac S, Cheng M, Tilghman SM. Quantitative trait loci that modify the severity of spotting in piebald mice. Genome Res. 1995; 5:29–41. [PubMed: 8717053]

Pingault V, Bondurand N, Kuhlbrodt K, Goerich DE, Prehu MO, Puliti A, Herbarth B, Hermans-Borgmeyer I, Legius E, Matthijs G, et al. SOX10 mutations in patients with Waardenburg-Hirschsprung disease. Nat Genet. 1998; 18:171–173. [PubMed: 9462749]

Potterf SB, Furumura M, Dunn KJ, Arnheiter H, Pavan WJ. Transcription factor hierarchy in Waardenburg syndrome: regulation of MITF expression by SOX10 and PAX3. Hum Genet. 2000; 107:1–6. [PubMed: 10982026]

Potterf SB, Mollaaghababa R, Hou L, Southard-Smith EM, Hornyak TJ, Arnheiter H, Pavan WJ. Analysis of SOX10 function in neural crest-derived melanocyte development: SOX10-dependent transcriptional control of dopachrome tautomerase. Dev Biol. 2001; 237:245–257. [PubMed: 11543611]

Pusch C, Hustert E, Pfeifer D, Sudbeck P, Kist R, Roe B, Wang Z, Balling R, Blin N, Scherer G. The SOX10/Sox10 gene from human and mouse: sequence, expression, and transactivation by the encoded HMG domain transcription factor. Hum Genet. 1998; 103:115–123. [PubMed: 9760192]

Ripoll VM, Meadows NA, Raggatt LJ, Chang MK, Pettit AR, Cassady AI, Hume DA. Microphthalmia transcription factor regulates the expression of the novel osteoclast factor GPNMB. Gene. 2008; 413:32–41. [PubMed: 18313864]

Sato-Jin K, Nishimura EK, Akasaka E, Huber W, Nakano H, Miller A, Du J, Wu M, Hanada K, Sawamura D, et al. Epistatic connections between microphthalmia-associated transcription factor and endothelin signaling in Waardenburg syndrome and other pigmentary disorders. FASEB J. 2008; 22:1155–1168. [PubMed: 18039926]

Southard-Smith EM, Angrist M, Ellison JS, Agarwala R, Baxevanis AD, Chakravarti A, Pavan WJ. The Sox10(Dom) mouse: modeling the genetic variation of Waardenburg-Shah (WS4) syndrome. Genome Res. 1999; 9:215–225. [PubMed: 10077527]

Southard-Smith EM, Kos L, Pavan WJ. Sox10 mutation disrupts neural crest development in Dom Hirschsprung mouse model. Nat Genet. 1998; 18:60–64. [PubMed: 9425902]

Steel KP, Davidson DR, Jackson IJ. TRP-2/DT, a new early melanoblast marker, shows that steel growth factor (c-kit ligand) is a survival factor. Development. 1992; 115:1111–1119. [PubMed: 1280558]

Steingrimsson E, Copeland NG, Jenkins NA. Melanocytes and the microphthalmia transcription factor network. Annu Rev Genet. 2004; 38:365–411. [PubMed: 15568981]

Tassabehji M, Newton VE, Read AP. Waardenburg syndrome type 2 caused by mutations in the human microphthalmia (MITF) gene. Nat Genet. 1994; 8:251–255. [PubMed: 7874167]

Tsujimura T, Morii E, Nozaki M, Hashimoto K, Moriyama Y, Takebayashi K, Kondo T, Kanakura Y, Kitamura Y. Involvement of transcription factor encoded by the mi locus in the expression of c-kit receptor tyrosine kinase in cultured mast cells of mice. Blood. 1996; 88:1225–1233. [PubMed: 8695840]

Verastegui C, Bille K, Ortonne JP, Ballotti R. Regulation of the microphthalmia-associated transcription factor gene by the Waardenburg syndrome type 4 gene, SOX10. J Biol Chem. 2000; 275:30757–30760. [PubMed: 10938265]

Walhout AJ. Unraveling transcription regulatory networks by protein-DNA and protein-protein interaction mapping. Genome Res. 2006; 16:1445–1454. [PubMed: 17053092]

Wilkinson, DG.; Nieto, MA. Detection of Messenger RNA by in Situ Hybridization to tissue Sections and Whole Mounts. In: Wassarman, PM.; DePamphilis, ML., editors. Methods in Enzymology: Guide to Techniques in Mouse Development. San Diego: Academic Press, Inc; 1993. p. 361-373.

Yasumoto K, Mahalingam H, Suzuki H, Yoshizawa M, Yokoyama K. Transcriptional activation of the melanocyte-specific genes by the human homolog of the mouse Microphthalmia protein. J Biochem. 1995; 118:874–881. [PubMed: 8749302]

Yasumoto K, Yokoyama K, Takahashi K, Tomita Y, Shibahara S. Functional analysis of microphthalmia-associated transcription factor in pigment cell-specific transcription of the human tyrosinase family genes. J Biol Chem. 1997; 272:503–509. [PubMed: 8995290]

Zhiqi S, Soltani MH, Bhat KM, Sangha N, Fang D, Hunter JJ, Setaluri V. Human melastatin 1 (TRPM1) is regulated by MITF and produces multiple polypeptide isoforms in melanocytes and melanoma. Melanoma Res. 2004; 14:509–516. [PubMed: 15577322]

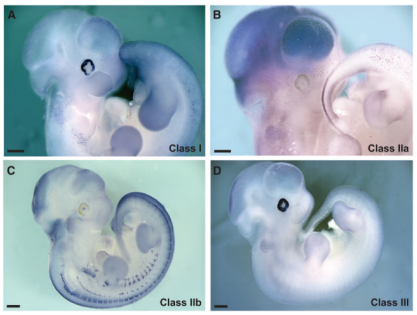

Figure 1. *In vivo* developmental expression profiles of pigment cell-expressed genes

The whole mount *in situ* patterns of expression allow categorization of the fourteen pigmentation genes into four lineage-restricted expression pattern groups. (A) Class I expression, represented by *Tyr*, displays a melanoblast- and RPE-positive pattern (*Mitf*, *Dct*, *Si*, *Gpnmb*, and *Slc45a2* data not shown). (B) Class IIa expression, represented by *Kit*, displays a melanoblast-positive, RPE-negative early PNS-negative pattern. (C) Class IIb expression, represented by *Ednrb*, displays a melanoblast-positive, RPE-negative, and early PNS-positive pattern (*Sox10* and *Erbb3* data not shown). (D) Class III expression, represented by *Trpm1*, displays a melanoblast-negative, RPE-positive pattern (*Rab38*, *Mlana and Tyrp1* data not shown). All images are of C57BL/6J, E11.5 embryos. Scale bars = 500μm. Data not shown is available at http://research.nhgri.nih.gov/manuscripts/Loftus/March2009/.

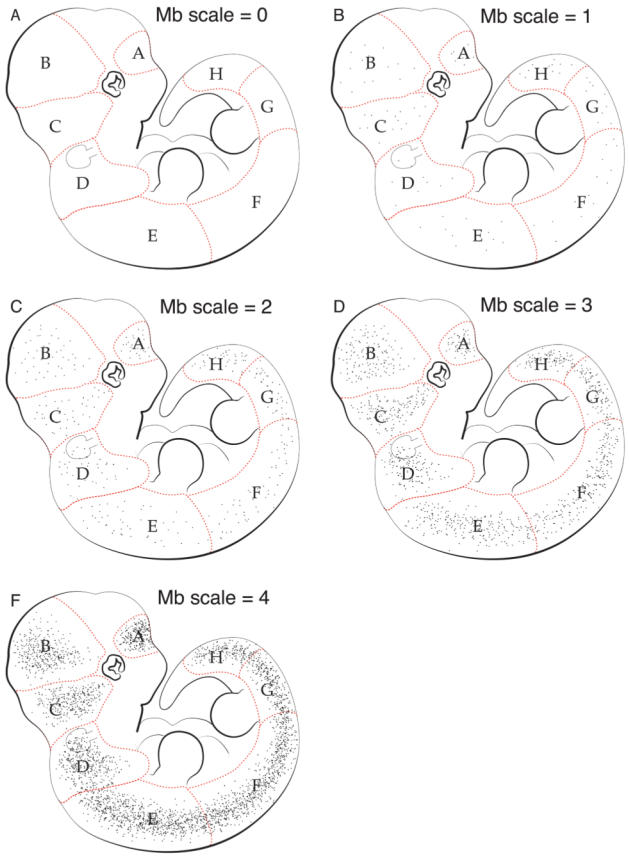

Figure 2. Embryonic Melanoblast Density Scale (MDS)

Graphical representation of the standardized MDS utilized to describe the pattern of *in situ* gene expression within eight defined regions of the mouse embryo. The eight regions are denoted by red dotted lines and labeled A-H in a rostral to caudal manner along E11.5 mouse embryos. Each region was scored independently for each embryo using a scale of 0–4 as defined by the following template images: (A) Mb scale =0, no expression. (B) Mb scale = 1, low expression corresponding to less than 12 positive cells within the region. (C) Mb scale =2, moderate number of melanoblasts, sparsely distributed. (D) Mb scale =3, even and numerous melanoblast positive cells. (E) Mb scale =4, extremely dense and overlapping pattern.

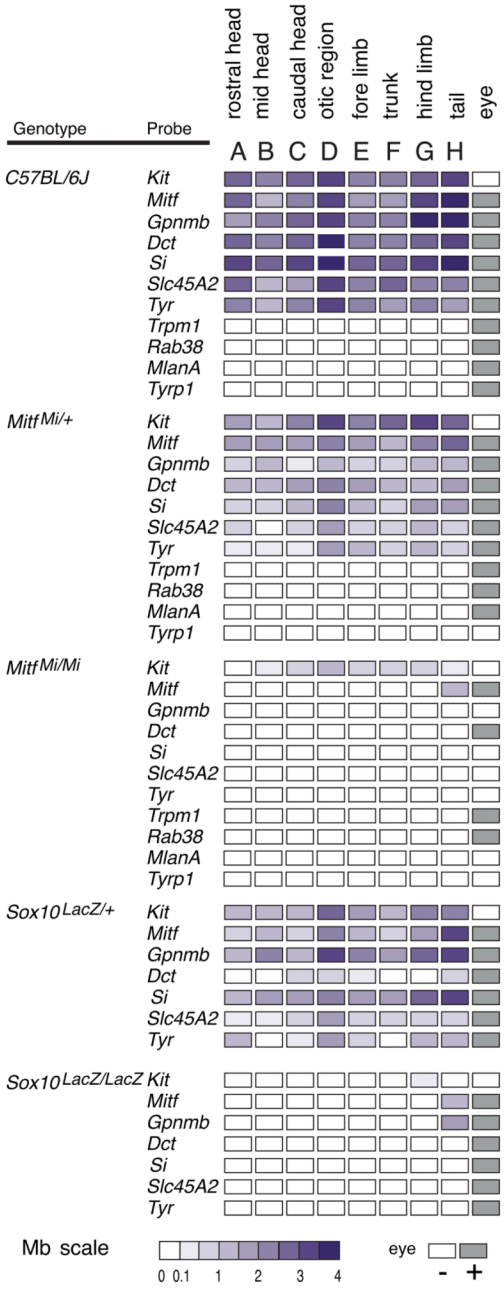

Figure 3. Transcription factor mutants subdivide *in vivo* pigment gene expression groups

The Mb-positive cell distribution scores for the Class I, IIa and III pigment cell-expressed genes are sorted by genotype and summarized by heatmap visualization. For each gene, 2 or more embryos were scored for both right and left sides using the MDS outlined in Figure 2. Then all MDS values for each gene were averaged and converted to a white=(0) to dark purple=(4) visualization gradient, indicating Mb cell density within a region. For Class I and IIa genes, expression was analyzed in C57BL/6J wildtype embryos and *Mitf* and *Sox10* transcription factor deficient embryos ($Mitf^{mi/+}$, $Mitf^{mi/mi}$ $Sox10^{tm1Weg/+}$, and $Sox10^{tm1Weg/tm1Weg}$, respectively) at E11.5. For Class III genes, which are only expressed in the RPE, analysis was performed on wildtype, $Mitf^{mi/+}$, and $Mitf^{mi/mi}$ embryos, as *Sox10* is

not expressed in the RPE. The presence of gene expression in the developing eye is denoted by grey, and the absence of expression by white in the far right column.

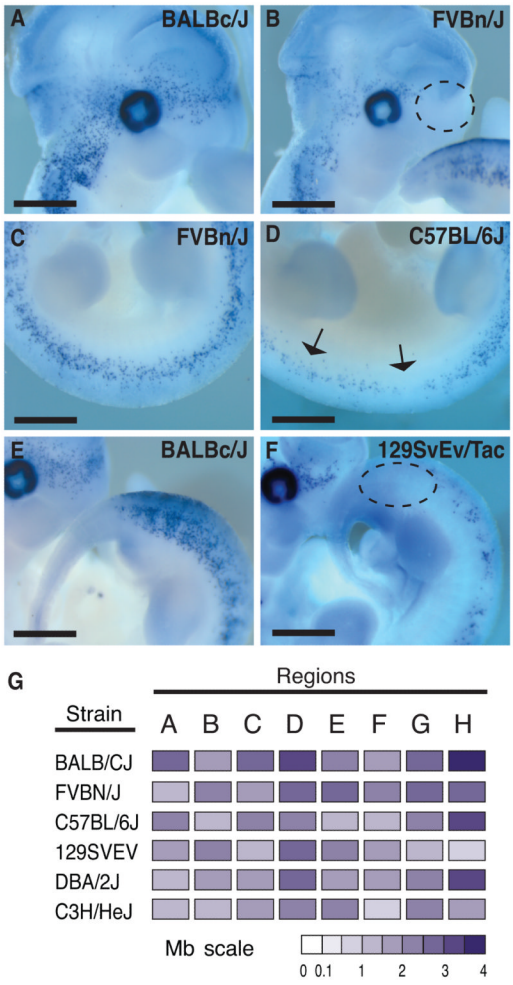

Figure 4. Regional variation in *Si* expression is dependant on inbred strain background

The number of *Si*-positive melanoblasts in an E11.5 embryo varies in both a region- and inbred strain-specific manner. Representative images illustrate the observed variation in *Si*-positive melanoblasts (panels A, B) at the boundary between the telencephalon and nasal process located in MDS region A; (panels C, D) the melanoblasts in the embryonic trunk within MDS region F and (panels E, G) melanoblasts in the distal tail within MDS region H. Regions in which *Si*-positive melanoblasts are absent/reduced are indicated by dotted lines. Arrows indicate areas within the trunk that display a localized reduction in melanoblast numbers. (panel G) MDS heatmap summary for numerical MDS values presented in Table 1 of *Si*-positive melanoblast expression by region for the six inbred strains indicated. N=4 embryos/strain. Scale bar =500μm.

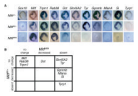

Figure 5. RPE-expressed gene groups are defined based upon modulation of MITF expression

A) Whole mount *in situ* RPE gene expression at E11.5 on wild-type (row 1), *Mitf*$^{mi/+}$ (row 2), and *Mitf*$^{mi/mi}$ (row 3) embryos. The eleven genes compared are annotated across the top of the columns. *Sox10* is not expressed in the RPE, and therefore allows visualization of the reduced pigmentation observed in the *Mitf*$^{mi/+}$ and *Mitf*$^{mi/mi}$ backgrounds. B) Variation in gene expression, in response to reduced functional MITF, further defines the expression of these eleven genes into five distinct MITF expression response categories. RPE Group 1: *Mitf*, *Rab38*, and *Trpm1*; RPE Group 2: *Dct*; RPE Group 3: *Slc45A2* and *Tyr*; RPE Group 4 *Gpnmb*, *Mlana*, and *Si*; and RPE Group 5: *Tyrp1*.

Table 1

Si- Melanoblast density score (MDS) varies by region (A-H) and with respect to inbred strain background

	A	B	C	D	E	F	G	H
Strain	**rostral head**	**midbrain- hindbrain boundary**	**caudal head**	**otic vessicle, CG IX**	**forelimb**	**trunk**	**hindlimb**	**tail**
129SvEv/Tac	1.63 +/− 0.72	2.00 +/− 0.97	* 1.50 +/− 0.52	2.80 +/− 1.01	1.94 +/− 0.77	1.63 +/− 0.62	* 1.63 +/− 0.72	* 0.94 +/− 0.85
BALB/cJ	* 2.5 +/− 0.63	2.00 +/− 0.37	* 2.94 +/− 0.68	* 3.44 +/− 0.63	2.38 +/− 0.62	1.63 +/− 0.62	* 2.69 +/− 0.60	* 3.69 +/− 0.48
C3H/HeJ	1.19 +/− 0.54	1.81 +/− 0.54	1.69 +/− 0.70	2.44 +/− 0.63	2.13 +/− 0.81	* 1.06 +/− 0.25	2.00 +/− 0.73	1.88 +/− 0.62
C57BL/6J	2.07 +/− 0.92	* 1.29 +/− 0.47	2.29 +/− 0.61	* 2.43 +/− 0.51	* 1.36 +/− 0.50	1.29 +/− 0.47	2.43 +/− 0.51	3.00 +/− 0.88
DBA/2J	* 1.06 +/− 0.25	1.94 +/− 0.68	1.81 +/− 0.66	2.50 +/− 0.63	1.94 +/− 0.44	1.81 +/− 0.54	2.31 +/− 0.79	3.00 +/− 0.63
FVB/NJ	1.13 +/− 0.62	* 2.38 +/− 0.62	1.94 +/− 0.68	2.69 +/− 0.60	* 2.56 +/− 0.63	* 2.31 +/− 0.70	2.63 +/− 0.50	2.81 +/− 0.66

* highest and lowest MDS value pair for each region